INTERFACIAL CHARACTERISATION AND OPTIMISATION OF CARBON NANOTUBE FIBRES

James Trevarthen*[1], Dawid Janas[2], Michael Wisnom[1], Sameer Rahatekar[1], Krzysztof Koziol[2]

[1] *Advanced Composite Centre for Innovation and Science, University of Bristol, Bristol, UK*
[2] *Department of Materials Science, University of Cambridge, Cambridge, UK*
* *Corresponding Author: james.trevarthen@bris.ac.uk*

Keywords: Interface, Nanocomposite, Carbon Nanotube

Abstract
Carbon nanotube fibres have the potential to reinforce high-performance polymer composites, but to do so will require an effective interface between fibre and matrix. Here we show that achieving such an interface is challenging using a conventional interfacial structure. Instead, we demonstrate the effectiveness of an alternative interfacial structure in a model composite that does not require aggressive chemistry. This results in a critical interfacial shear stress of 50.5 MPa whilst maintaining adhesion beyond 10% strain.

1. Introduction

The development of strong, stiff carbon nanotube (CNT) fibres (CNTF) with specific mechanical properties comparable to conventional reinforcement fibres [1, 2] presents the possibility of producing a new generation of high performance composites. Moreover these fibres have further advantages, such as their conductivity [3], potential for high strain to failure and ductility [4], and in some cases, continuous production from simple, low-cost precursors [1, 2].

However, to produce high performance CNTF/polymer composites a high-performance fibre-matrix interface is required. Early studies of CNTF/Polymer composites showed that interfacial performance was limiting [5, 6]. This is attributed to two factors: firstly, poor chemical compatability at the interface, and secondly, the partial infiltration of the porous CNTF structure by the matrix during composite manufacture. Partial infiltration increases CNT/matrix interfacial area, which might be thought to be favourable for stress-transfer. However, unless infiltration is complete the result is a cross-sectional structure where a dry core of fibre is surrounded by an infiltrated shell. It is believed that stress transfer and adhesion across this secondary internal interface is very poor, leading to premature debonding or slip in this zone [6].

The performance of an interface is controlled by a combination of interfacial morphology and the chemical compatibility of fibre and matrix. In this study we investigate the surface chemistry of the fibres to demonstrate the difficulty of achieving good interfacial performance using the conventional reinforcement fibre approach of surface functionalisation and sizing. To overcome this difficulty we explore an alternative interfacial structure exploiting CNTF morphology with potential to yield a high performance interface.

2. Fibre Surface Analysis

Interfacial adhesion is defined at the molecular level by the density and type (Lifschitz-van der Waals or acid-base) of interactions between fibre and matrix. Fibre-matrix compatability can be described by an interfacial energy (γ_{fm}), which is a function of the surface energies of fibre and matrix (γ_f, γ_m), or more specifically the components of surface energy attributed to Lifschitz-van der Waals (γ_f^{LW}, γ_m^{LW}) and acid-base (γ_f^+, γ_f^-; γ_m^+, γ_m^-) interactions [7].

Whilst adhesion is complex, for best interfacial performance it is generally desirable to have a large fibre surface energy, with contributions approximately matched to the corresponding contributions of the matrix: $\gamma_f^{LW} \approx \gamma_m^{LW}$, $\gamma_f^+ \approx \gamma_m^-$, $\gamma_f^- \approx \gamma_m^+$.

Measurement of γ_f and estimation of its contributions therefore allows comparison with values for different fibres and matrix materials to estimate interfacial favourability. It also informs surface functionalisation, by suggesting what kind of surface chemistry should be introduced: for example adding basic groups to increase γ_f^+.

2.1. Surface energy measurement procedure

Contact angles were measured using a *Krüss* K100 Tensiometer according to the method described by Hsieh and Yu [8]. Due to their small diameter, it was not possible to obtain accurate measurements for CNTF. Instead their chemically analogous precursor, CNT sheets (CNTS), were used. CNTS were produced according to the method described in [2].

CNTS solid surface energy (γ_{CNTS}) was estimated using the Zisman method [9]. A plot of surface tensions of various probe liquids, γ_{lv}, are plotted against the cosines of their contact angles with CNTS. The value of γ_{CNTS} is taken as the value of γ_{lv} at which the curve diverges from the line $\cos\theta = 1$. Values of γ_{lv} were measured using a *Krüss* K100 Tensiometer according to the Wilhelmy plate method [10], using a PtIr plate. A list of probe liquids, their purities and suppliers can be found in Table 2.2.

2.2. Results and discussion

Probe Liquid	**Supplier**	**Purity [%]**	γ_l **[J/mm^2]**	$\cos\theta$
N,N DMF	Sigma Aldrich	99.8	37.3 (0.10)	0.92 (0.04)
DMSO	Fisher Scientific	> 99	43.6 (0.01)	0.72 (0.03)
n-Hexane	Sigma Aldrich	99	18.4 (0.02)	1 (-)
Ethylene glycol	Sigma Aldrich	99.8	48.8 (0.06)	0.59 (0.06)
Toluene	Sigma Aldrich	99.8	26.1 (0.07)	0.99 (0.03)
Ethanol	Sigma Aldrich	≥ 99.5	22.4 (0.03)	0.98 (0.01)

Table 1. Provenance and purity of probe liquids used, their experimentally determined surface energies and cosines of contact angles with CNTS. Standard deviations of experimental values are shown in parentheses.

Surface energy was determined to be 34.6 mN/m (Figure 1). Due to the graphitic, sp^2 hybridised CNT surface it can be assumed that $\gamma_f^{LW} \approx \gamma_f$ and $\gamma_f^+ \approx \gamma_f^- \approx 0$. This value is low relative to conventional reinforcement fibre surface energies [11], and not compatible with typical matrix materials, which typically have larger surface energy and a significant acidic or basic

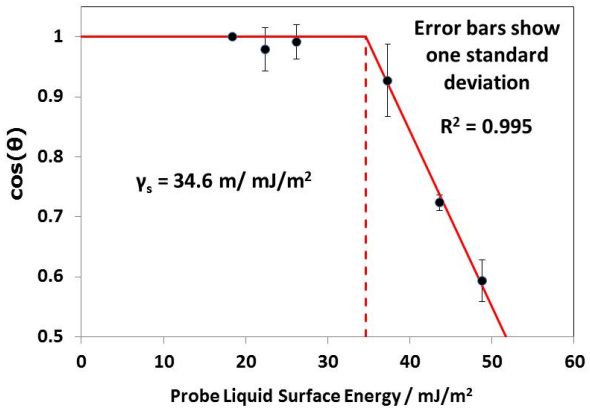

Figure 1. A Zisman plot of $\cos\theta$ vs. γ_l for different probe liquids in contact with CNTS. The value of γ_{CNTS} is found to be 34.6 mJ/m^2. Error bars show standard error.

contribution [12]. This result agrees with the hypothesis that CNT fibre chemistry is a cause of limited interfacial performance observed in the literature.

The conventional solution to low surface energy is typically a combination of chemical functionalisation of the surface (carbon fibre: oxidation, glass fibre: silanisation) and a polymer coating (sizing). However, chemical functionalisation of CNTF is problematic as, due to the chemical stability of the aromatic CNT structure, sufficient functionalisation may require aggressive treatments or long process times [13].

An alternative to surface treatment is to exploit the large available surface area of CNT fibres by totally infiltrating them with the parent matrix. The low favourability of the interface per unit area is therefore overcome by creating a very large interfacial area. This may also eliminate core-shell failure by removing the presence of this weak interface.

3. An Alternative, Infiltrated Interfacial Structure

Having identified extensive fibre infiltration as an alternative to surface treatment, it is now necessary to demonstrate its effectiveness. In practice, achieving extensive infiltration with conventional engineering resins can be problematic due to their high viscosity. Instead, we use a low viscosity solution of polycarbonate (PC) to infiltrate fibres. PC is used as a model matrix due to its solubility in common solvents and moderate mechanical properties as well as its high optical clarity and birefringence, useful in interfacial performance characterisation.

The infiltration of fibres also has the potential to reduce their mechanical properties by causing misalignment of CNTs or reduced stress-transfer within the fibre. To characterise the effect of infiltration, fibre strengths are measured both with and without polymer infiltration.

It is also necessary to quantify the performance of the infiltrated interface. This is characterised in terms of both stress transfer efficiency and how adhesion is maintained under loading. For comparison, T300 carbon fibre interfacial performance is also characterised.

Stress transfer occurs through shear stress at the fibre-matrix interface. The simplest stress-transfer model is that of Kelly and Tyson [14] (Eqn. 1), which is still widely used [15]. It

defines stress transfer efficiency using the critical interfacial shear stress, τ_i^*, which is a function of fibre strength, σ_f^*, fibre diameter, d and the critical fragment length, l_c. The value of l_c is defined in numerous ways [16]. Here the simplest definition is used; l_c is the mean saturation length of fibre fragments in a composite sample after loading.

$$\tau_i^* = \frac{\sigma_f^* d}{2 l_c} \tag{1}$$

Numerous methods exist for measuring l_c [17]. The single fibre fragmentation test (SFFT) is used here as it most accurately models the conditions in a composite, with the additional benefit of allowing observation of the progression of interfacial damage with increasing strain.

3.1. Experimental procedure

To achieve fibre infiltration, a dilute (1 wt%) solution of PC in tetrahydrofuran (THF) was prepared in which CNTF were immersed before removal and solvent evaporation. Fibres were held taut to maintain CNT alignment. Diameters of fibres were measured before and after infiltration using a *Zeiss* AxioVision M2 optical microscope.

Fibre mechanical properties were tested according to ASTM C1557 [18] using an *Instron* 3343 load frame fitted with a 10N load cell. A gauge length of 5mm and a crosshead extension rate of 0.35 mm min^{-1} were used. Fibre diameters were measured pre-test using a *Zeiss* AxioVision M2 optical microscope.

CNTF were produced according to the method described in [2]. It should be noted that, in order to minimise fibre synthesis burden, fibres of moderate mechanical performance were used in this experiment to serve as a model system for higher performance CNTF.

SFF test protocol was designed from published methods [19, 17]. Fibres were mounted on pre-cut PC dogbone substrates of 0.175 mm thickness with gauge length and width of 16mm and 5mm respectively. A thin coating of PC was applied by solution casting from THF. Fibre diameters were measured *in situ* prior to test using a *Zeiss* AxioVision M2 optical microscope. SFF testing was carried out on a *Deben* micro-tensile test stage mounted between two crossed linear polarisers in a *Zeiss* AxioVision M2 optical microscope to observe. Extension was applied at 0.2 mm min^{-1} in increments of 0.1mm. After each increment sample extension was measured and fibre fractures, identified using birefringence patterns, were counted.

Because of specimen necking at high strain, CNTF fragment lengths were measured only in regions where fragmentation was saturated according to the method described by Pisanova [20].

3.2. Results and Discussion

3.2.1. Fibre Mechanical Properties

Mean fibre strengths of CNTF with and without PC infiltration are shown in Figure 2. As discussed earlier, fibres used were not of the highest mechanical performance in order to minimise

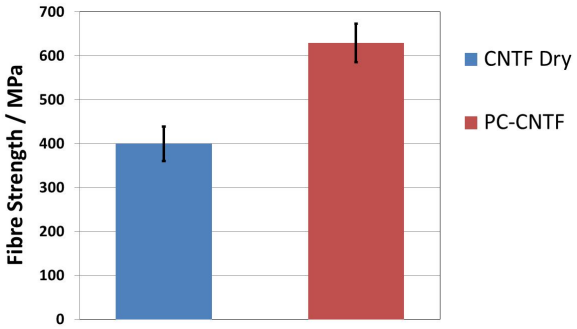

Figure 2. Mean fibre strengths with and without PC infusion, showing a large increase when fibres are infiltrated. This is attributed to stabilisation of CNT slip by the polymer. Error bars show one standard error.

experimental burden. The effect of PC infiltration is an average strength increase of 57%, without any statistically significant change in fibre diameter due to infiltration. The strength increase is attributed to the stabilisation of CNT-CNT slip, the suspected failure mechanism of CNTF, and increased condensation improving CNT-CNT stress transfer. Increased fibre condensation is believed to be caused by capillary action during THF evaporation [21]. Strength improvement may be counteracted by increased linear density, resulting in a less significant change in specific strength. A vibrometric study of fibre linear density is currently in progress to assess this effect and estimate the quantity of infiltrated polymer.

The test equipment used did not yield stiffness or strain to failure results. Further work is underway to determine the effect of infiltration on stiffness and strain-to-failure, as well as to confirm the extent of fibre infiltration.

3.2.2. Single Fibre Fragmentation

Fibre	**Fragmentation Onset Strain [%]**	**Fragmentation Sat'n Strain [%]**	**Fragment Length [μm]**	τ_i^* **[MPa]**
T300	1.88	3.42	1164.0 (0.3)	12.4
CNTF	3.15	>10.00	55.7 (6.5)	50.5

Table 2. Mean fragmentation onset and saturation strains and mean fragment lengths and critical interfacial shear stresses for T300 and CNTF. T300 fragmentation onsets and reaches saturation much earlier than CNTF, demonstrating the higher strain capability of CNTF. The higher critical interfacial shear stress also shows interfacial stress transfer is more efficient for CNTF than T300.

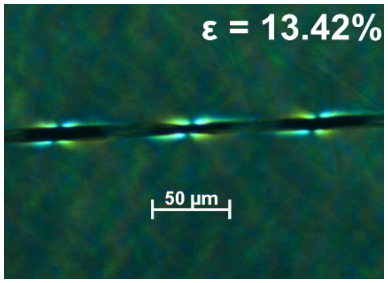

Figure 3. Birefringence patterns around three CNTF fragments at 13.42% strain, showing strong birefringence patterns, indicating continued adhesion at very high strain. Birefringence patterns were not observed to change with strain, indicating minimal debonding.

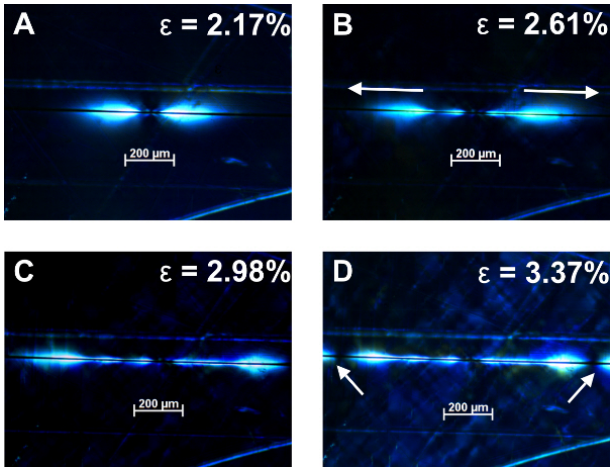

Figure 4. Birefringence patterns at a T300 fibre break at different strains. A: Post-fracture, strong fringes show efficient stress transfer with no debonding. B: Fibre debonding begins. C: Debond propagates, decreasing effective length of fibre. D: Fibre fragments almost entirely debonded as debonds from either end of fragments meet.

During single fibre fragmentation testing, both CNTF and T300 fragmented extensively, showing sufficient stress transfer efficiency to load fibres to failure. Table 2 shows mean fragmentation onset and saturation strains for both fibres. T300 fragmentation onsets at a considerably lower strain than CNTF, due to the higher failure strains, as observed in the literature. An exact saturation strain for CNTF was not observed as the matrix began to neck before fragmentation saturation, preventing accurate prediction of local strains at which fragmentation occurred. However, fragmentation was observed to continue occurring at global strains above 10%. This longer interval of fragmentation demonstrates more graceful development of damage.

Table 2 shows mean fragment lengths observed for T300 and CNTF and the associated values of τ_i^*, demonstrating that CNTF performs significantly better than T300. The value of τ_i^* measured for CNTF is high, lying between published values of PC yield and ultimate shear strengths [22].

Additionally, it was observed that adhesion between CNT fibre and matrix was maintained even at very high global strains (> 10%) with neither debonding nor propagation of plastic yield at the interface observed, up to the point of tensile matrix failure. This is shown in Figure 3, where strong birefringence patterns are observed around 3 CNTF fragments, showing continued strong adhesion at a global strain of 13.42%. This contrasts with T300, for which debonding occurred soon after fragmentation onset, as illustrated in Figure 4, showing the progression of interfacial debonding with increased strain.

The extremely small CNTF value of l_c may increase fibre performance as high performance CNTF have been shown in the literature to have dramatically increased performance when gauge length is reduced from 20mm to 1mm, with evidence of a shift in failure mode [1]. As the critical length observed here is much lower than 1mm, it is therefore believed that this short gauge performance would be observed in CNTF composites with this interfacial structure.

The results of this study show that it is possible to achieve a high performance CNTF/Polymer interface by careful consideration of interface morphology, offering the possibility of exploiting the mechanical and functional performance of CNTF in polymer composites.

4. Conclusion

Due to their porous structure and the low surface energy measured here, the case is made that forming an effective CNTF/polymer interface with a traditional interfacial architecture is likely to result in poor performance, as observed in the literature.

Instead, we demonstrate a model interface exploiting the large accessible surface area of the fibre by extensive matrix infiltration. This interfacial structure is shown to improve fibre strength by 57%. The resulting interfacial performance is also significantly better than that of commercially sized and oxidised T300 in PC, showing an interfacial shear strength of 50.5 MPa, with adhesion maintained at very large strains (>10%).

Whilst further work is needed to confirm the extent of fibre infiltration, as well as its effect on fibre stiffness and strain to failure, this interfacial structure represents a possible route to CNTF exploitation as a composite reinforcement. This work is currently being extended to ductile CNTF, with the intention of producing ductile CNTF/polymer composites.

Acknowledgements

This research was supported by the EPSRC, through the CDT for Advanced Composites Innovation and Science (Grant no. EP/G036772/1) and Programme Grant EP/I02946X/1 on High Performance Ductile Composite Technology in collaboration with Imperial College, London.

References

[1] K.K. Koziol, J. Vilatela, A. Moisala, M. Motta, P. Cunniff, M. Sennett, and A. Windle. High-performance carbon nanotube fiber. *Science*, 318(5858):1892–5, 2007.

[2] Y.-L. Li, I.A. Kinloch, and A.H. Windle. Direct spinning of carbon nanotube fibers from chemical vapor deposition synthesis. *Science*, 304(5668):276–8, 2004.

[3] T.-W. Chou, L. Gao, E.T. Thostenson, Z. Zhang, and J.-H. Byun. An assessment of the science and technology of carbon nanotube-based fibers and composites. *Composites Science and Technology*, 70(1):1–19, 2010.

[4] S. Boncel, R.M. Sundaram, A.H. Windle, and K.K. Koziol. Enhancement of the mechanical properties of directly spun CNT fibers by chemical treatment. *ACS nano*, 5(12):9339–44, 2011.

[5] F. Deng, W. Lu, H. Zhao, Y. Zhu, B.-S. Kim, and T.-W. Chou. The properties of dry-spun carbon nanotube fibers and their interfacial shear strength in an epoxy composite. *Carbon*, 49(5):1752–1757, 2011.

[6] M. Zu, Q. Li, Y. Zhu, M. Dey, G. Wang, W. Lu, J.M. Deitzel, J.W. Gillespie, J.-H. Byun, and T.-W. Chou. The effective interfacial shear strength of carbon nanotube fibers in an epoxy matrix characterized by a microdroplet test. *Carbon*, 50(3):1271–1279, 2012.

[7] C.J. Van Oss, M.K. Chaudhury, and R.J. Good. Interfacial Lifshitz-van der Waals and polar interactions in macroscopic systems. *Chemical Reviews*, 88(6):927–941, 1988.

[8] Y.-L. Hsieh and B. Yu. Liquid Wetting, Transport, and Retention Properties of Fibrous Assemblies: Part I: Water Wetting Properties of Woven Fabrics and Their Constituent Single Fibers. *Textile Research Journal*, 62(11):677–685, 1992.

[9] W.A. Zisman. Relation of the Equilibrium Contact Angle to Liquid and Solid Constitution. In *Advances in Chemistry, Volume 43*, pages 1–51. American Chemical Society, 1964.

[10] K. Holmberg, D. O. Shah, and M. J. Schwuger. *Handbook of Applied Surface and Colloid Chemistry*. 2002.

[11] M.Q. Tran, K.K.C. Ho, G. Kalinka, M.S.P. Shaffer, and A. Bismarck. Carbon fibre reinforced poly (vinylidene fluoride): impact of matrix modification on fibre/polymer adhesion. *Composite Science and Technology*, 8(2009):7–8, 2008.

[12] C. Della Volpe and S. Siboni. Some Reflections on Acid Base Solid Surface Free Energy Theories. *Journal of Colloid and Interface Science*, 195(1):121–136, 1997.

[13] P. Ma, N.A. Siddiqui, G. Marom, and J. Kim. Dispersion and functionalization of carbon nanotubes for polymer-based nanocomposites: A review. *Composites Part A: Applied Science and Manufacturing*, 41(10):1345–1367, 2010.

[14] A. Kelly and W.R. Tyson. Tensile properties of fibre-reinforced metals: copper/tungsten and copper/molybdenum. *Journal of the Mechanics and Physics of Solids*, 13:329 – 350, 1965.

[15] S.F. Zhandarov and E.V. Pisanova. Two interfacial shear strength calculations based on the single fiber composite test. *Mechanics of Composite Materials*, 31(4):325–336, 1995.

[16] S.F. Zhandarov, E.V. Pisanova, and V.A. Dovgyalo. Fragmentation of a single filament during tension in a matrix as a method of determining adhesion. *Mechanics of Composite Materials*, (3), 1992.

[17] M.J. Pitkethly, J. Jakubowski, S.F. Mudrich, D.L. Caldwell, L.T. Drzal, L. Di Landro, A. Hampe, J.P. Armistead, M. Desaeger, and I. Verpoest. A round-robin programme on interfacial test methods. *Composites Science and Technology*, 48:205–214, 1993.

[18] ASTM Standard C1557, 2003 (2008), "Tensile Strength and Young's Modulus of Fibers", ASTM International, West Conshohocken, Pennsylvania, 2008, DOI: 10.1520/C1557-03R08, www.astm.org.

[19] S. Feih, K. Wonsyld, D. Minzari, P. Westermann, and H. Lilholt. Testing Procedure for the Single Fiber Fragmentation Test. Technical report, Riso National Laboratory, 2004.

[20] E V Pisanova, F Zhandarov, and V A Dovgyalo. Single Filament Thermoplastic Composites. *Polymer Composites*, 15(2):147–155, 1994.

[21] S. Li, X. Zhang, J. Zhao, F. Meng, G. Xu, Z. Yong, J. Jia, Z. Zhang, and Q. Li. Enhancement of carbon nanotube fibres using different solvents and polymers. *Composites Science and Technology*, 72(12):1402–1407, 2012.

[22] C. G'Sell and A.J. Gopez. Plastic banding in glassy polycarbonate under plane simple shear. *Journal of Materials Science*, 20(155):3462–3478, 1985.